

Energy Transfer Pathways in Dinuclear Heteroleptic Polypyridyl Complexes: Through-Space vs Through-Bond Interaction Mechanisms

Frances Weldon,[†] Leif Hammarström,[‡] Emad Mukhtar,[‡] Ronald Hage,[§] Eric Gunneweg,^{||} Jaap G. Haasnoot,^{||} Jan Reedijk,^{||} Wesley R. Browne,^{†,⊥} Adrian L. Guckian,[†] and Johannes G. Vos^{*†}

National Centre for Sensor Research, School of Chemical Sciences, Dublin City University, Dublin 9, Ireland, Department of Physical Chemistry, University of Uppsala, Box 579, SE-75123, Sweden, Unilever R&D Vlaardingen, Olivier van Noortlaan 120, 3133 AT, Vlaardingen, The Netherlands, and Leiden Institute of Chemistry, Gorlaeus Laboratories, P.O. Box 9502, 2300 RA Leiden, The Netherlands

Received January 27, 2004

A series of homo- and heteronuclear ruthenium and osmium polypyridyl complexes with the bridging ligands 1,3-bis(5-(2-pyridyl)-1H-1,2,4-triazol-3-yl)benzene (H₂mL) and 1,4-bis(5-(2-pyridyl)-1H-1,2,4-triazol-3-yl)benzene (H₂pL) are reported. The photophysical properties of these compounds are investigated, and particular attention is paid to the heteronuclear (RuOs) compounds, which exhibit dual emission. This is in contrast to phenyl-bridged polypyridine Ru–Os complexes with a similar metal–metal distance, in which the Ru emission is strongly quenched because the nature of the bridging ligand allows for an efficient through-bond coupling. The results obtained for the compounds reported here suggest that energy transfer is predominantly taking place via a dipole–dipole, Förster type, mechanism, that may dominate when through-bond coupling is weak. This is in stark contrast to ground state interaction, which is found to be critically dependent on the nature of the bridging unit employed.

Introduction

The design and synthesis of multicomponent systems such as polynuclear metal complexes containing electroactive and photoactive units are topics of great current interest, not only in terms of fundamental studies of energy and electron transfer processes but also due to the potential of multicomponent systems as building blocks for supramolecular assemblies, molecular devices, and electroluminescent displays.^{1–5} Central to the development of multicomponent devices is the role of the bridging units employed in connecting active units and an understanding of the true role played by these bridges in mediating energy/electron transfer processes. In the case

of multinuclear transition metal complexes, the crucial role played by the bridging ligand in determining the ground state metal–metal interaction is already well recognized,⁶ with multinuclear systems employing imidazole,⁷ pyrazine,⁸ and ortho-metalated phenyl⁹ containing bridging units attracting

* Author to whom correspondence should be addressed. E-mail: Johannes.Vos@dcu.ie. Tel: 00353-1-7005307. Fax: 00353-1-7005503.

[†] Dublin City University.

[‡] University of Uppsala.

[§] Unilever R&D Vlaardingen.

^{||} Leiden Institute of Chemistry, Gorlaeus Laboratories.

[⊥] Present address: Organic & Molecular Inorganic Chemistry, Royal University Groningen, The Netherlands.

(1) (a) Worl, L. A.; Strouse, G. F.; Younathan, J. N.; Baxter, S. M.; Meyer, T. J. *J. Am. Chem. Soc.* **1990**, *112*, 7571. (b) Balzani, V. *Tetrahedron* **1992**, *48*, 10443. (c) Balzani, V.; Campagna, S.; Denti, G.; Juris, A.; Serroni, S.; Venturi, M. *Acc. Chem. Res.* **1998**, *31*, 26. (d) Balzani, V.; Scandola, F. *Supramolecular Photochemistry*; Horwood: Chichester, U.K., 1991. (e) Scandola, F.; Indelli, M. T.; Chiorboli, C.; Bignozzi, C. A. *Top. Curr. Chem.* **1990**, *158*, 73.

(2) (a) Kalyanasundaram, K. *Coord. Chem. Rev.* **1982**, *46*, 159. (b) Lehn, J. M. *Angew. Chem., Int. Ed. Engl.* **1988**, *27*, 89. (c) Balzani, V.; Campagna, S.; Denti, G.; Juris, A.; Serroni, S.; Ventura, M. *Coord. Chem. Rev.* **1994**, *132*, 1. (d) Balzani, V.; Juris, A.; Venturi, M.; Campagna, S.; Serroni, S. *Chem. Rev.* **1996**, *96*, 759. (e) Slate, C. A.; Striplin, D. R.; Moss, J. A.; Chen, P.; Erickson, B. W.; Meyer, T. J. *J. Am. Chem. Soc.* **1998**, *120*, 4885. (f) Hu, Y.-Z.; Tsukiji, S.; Shinkai, S.; Oishi, S.; Hamachi, I. *J. Am. Chem. Soc.* **2000**, *122*, 241. (g) Sauvage, J.-P.; Collin, J.-P.; Chambron, J.-C.; Guillerez, S.; Coudret, C.; Balzani, V.; Bargelletti, F.; De Cola, L.; Flamigni, L. *Chem. Rev.* **1994**, *94*, 993. (h) Carraway, E. R.; Demas, J. N.; DeGraff, B. A. *Anal. Chem.* **1991**, *63*, 332.

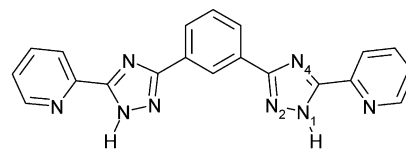
(3) (a) Balzani, V. Ed. *Supramolecular Photochemistry*; Reidel: Dordrecht, 1997. (b) Lehn, J.-M. *Supramolecular Chemistry*; Wiley-VCH: Weinheim, 1995.

(4) (a) Beer, P. D.; Szemes, F.; Balzani, V.; Salà, C. M.; Drew, M. G. B.; Dent, S. W.; Maestri, M. *J. Am. Chem. Soc.* **1997**, *119*, 11864. (b) Barigelletti, F.; Flamigni, L.; Collin, J.-P.; Sauvage, J.-P. *Chem. Commun.* **1997**, 333. (c) Waldmann, O.; Hassmann, J.; Müller, P.; Hanan, G. S.; Volkmer, D.; Schubert, U. S.; Lehn, J.-M. *Phys. Rev. Lett.* **1997**, *78*, 3390. (d) Zahavy, E.; Fox, M. A. *Chem. Eur. J.* **1998**, *4*, 1647. (e) Balzani, V.; Credi, A.; Venturi, M. *Curr. Opin. Chem. Biol.* **1997**, *1*, 506.

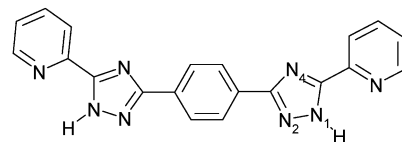
(5) Welter, S.; Brunner, K.; Hofstraat, J. W.; De Cola, L. *Nature* **2003**, *421*, 54.

considerable attention. In contrast, however, the role of bridging ligands in mediating excited state interaction has received less attention, especially as regards the relative importance of the Förster and Dexter mechanisms of energy transfer.

In recent years, the role of bridging ligands based on the 1,2,4-triazolato anion (e.g., 3,5-bis(2-pyridyl)-1*H*-1,2,4-triazolato, bpt^-) in mediating ground state interaction (i.e., the degree of delocalization of the singly occupied molecular orbital of the mixed valence complex ($\text{M}^{\text{II}}\text{M}^{\text{III}}$) over the metal centers) has been examined extensively. 1,2,4-Triazolato anion based ligands hold significant advantages over other bridging systems, due to the possibility of both the formation of coordination isomers and an accessible acid/base chemistry, which enable both synthetic and environmental manipulation of the photochemical and photophysical properties of Ru(II) and Os(II) homo- and heterometallic complexes incorporating these ligands.^{10–13} Indeed it is clear from these studies that ground state interaction between metal centers in the dinuclear complexes is mediated by the bridge through a hole transfer HOMO assisted superexchange mechanism.



1,3-bis(5-(2-pyridyl)-1*H*-1,2,4-triazol-3-yl)benzene (H_2mL)



1,4-bis(5-(2-pyridyl)-1*H*-1,2,4-triazol-3-yl)benzene (H_2pL)

Figure 1. Structures of the ligands H_2mL and H_2pL .

A further important attribute of these systems is the ability to modify excited state properties independently of the ground state metal–metal interaction, a feature that is essential to the development of multicomponent systems exhibiting rationally designed properties. As with other systems (vide supra) the nature of the mechanisms responsible for excited state energy transfer in these systems has received much less attention.

In this contribution the synthesis, characterization, and physical properties of a series of mononuclear and dinuclear Ru(II) and Os(II) complexes containing the ligands H_2mL and H_2pL (Figure 1) are described. Earlier electrochemical and spectroelectrochemical studies have demonstrated that in the ground state metal–metal interaction takes place via a hole transfer mechanism and this interaction can be tuned by changing structural features of the bridging ligand, such as meta vs para substitution.¹² Importantly the ground state interaction in these systems is critically dependent on the protonation state of the ligand. The aim of this study is to investigate the role these same structural parameters and the protonation state play in excited state interaction.

Experimental Section

Materials. All solvents employed were of HPLC grade or better and used as received unless otherwise stated. All reagents employed

- (6) (a) Barigelletti, F.; Flamigni, L.; Balzani, V.; Collin, J.-P.; Sauvage, J.-P.; Sour, A.; Constable, E. C.; Cargill Thompson, A. M. W. *J. Chem. Soc., Chem. Commun.* **1993**, 942. (b) Kim, Y.; Lieber, C. M. *Inorg. Chem.* **1989**, *28*, 3990.
- (7) (a) Haga, M.; Ano, T.; Kano, K.; Yamabe, S. *Inorg. Chem.* **1991**, *30*, 3843. (b) Haga, M. A.; Ishizuya, M.; Kanesugi, T.; Yubaka, T.; Sakiyama, D.; Fees, J.; Kaim, W. *Indian J. Chem. A* **2003**, *42*, 2290. (c) Haga, M.; Takasugi, T.; Tomie, A.; Ishizuga, M.; Yamada, T.; Hossain, M. D.; Inoue, M. *Dalton* **2003**, 2069. (d) Hossain, M. D.; Haga, M.; Gholamkhash, B.; Nozaki, K.; Tsushima, M.; Ikeda, N.; Ohno, T. *Collect. Czech. Chem. Commun.* **2001**, *66*, 307. (e) Hossain, M. D.; Ueno, R.; Haga, M. *Inorg. Chem. Commun.* **2000**, *3*, 35. (f) Ali, M.; Sato, H.; Haga, M. A.; Tanaka, K.; Yoshimura, A.; Ohno, T. *Inorg. Chem.* **1998**, *37*, 6176. (g) Haga, M.; Ali, M. M.; Sato, H.; Monjushiro, H.; Nozaki, K.; Kano, K. *Inorg. Chem.* **1998**, *37*, 2320. (h) Mizushima, K.; Nakaura, M.; Park, S. B.; Nishiyama, H.; Monjushiro, H.; Haraja, K.; Haga, M. *Inorg. Chim. Acta* **1997**, *261*, 175. (i) Haga, M. A.; Ali, M. M.; Koseki, S.; Fujimoto, K.; Yoshimura, A.; Nozaki, K.; Ohno, T.; Nakajima, K. *Inorg. Chem.* **1996**, *35*, 3335. (j) Haga, M. A.; Ali, M.; Arakawa, R. *Angew. Chem., Int. Ed. Engl.* **1996**, *35*, 76.
- (8) (a) Su, H. Q.; Kincaid, J. R. *J. Raman Spectrosc.* **2003**, *34*, 907. (b) Marcaccio, M.; Paolucci, F.; Paradisi, C.; Roffia, S.; Fontanesi, C.; Yellowlees, L. J.; Serroni, S.; Campagna, S.; Denti, G.; Balzani, V. *J. Am. Chem. Soc.* **1999**, *121*, 10081. (c) Loiseau, F.; Serroni, S.; Campagna, S. *Collect. Czech. Chem. Commun.* **2003**, *68*, 1677. (d) Marcaccio, M.; Paolucci, F.; Paradisi, C.; Carano, M.; Roffia, S.; Fontanesi, C.; Yellowlees, L. J.; Serroni, S.; Campagna, S.; Balzani, V. *J. Electroanal. Chem.* **2002**, *532*, 99. (e) Campagna, S.; Serroni, S.; Puntoriero, F.; Loiseau, F.; De Cola, L.; Kleverlaan, C. J.; Becher, J.; Sorenson, A. P.; Hascoat, P.; Thorup, N. *Chem. Eur. J.* **2002**, *8*, 4461. (f) Swavey, S.; Brewer, K. J. *Inorg. Chem.* **2002**, *41*, 4044. (g) Baudin, H. B.; Davidsson, J.; Serroni, S.; Juris, A.; Balzani, V.; Campagna, S.; Hammarstrom, L. *J. Phys. Chem. A* **2002**, *106*, 4312. (h) Seneviratne, D. S.; Uddin, J.; Swayambunathan, V.; Schegel, H. B.; Endicott, T. F. *Inorg. Chem.* **2002**, *41*, 1502. (i) Constable, E. C.; Eriksson, H.; Housecroft, C. E.; Kariuki, B. M.; Nordlander, E.; Olsson, J. *Inorg. Chem. Commun.* **2001**, *4*, 749. (j) Carano, M.; Ceroni, P.; Fontanesi, C.; Marcaccio, M.; Paolucci, F.; Paradisi, C.; Roffia, S. *Electrochim. Acta* **2001**, *46*, 3199. (k) Puntoriero, F.; Serroni, S.; Licciardello, A.; Venturi, M.; Juris, A.; Ricevutto, V.; Campagna, S. *Dalton* **2001**, 1035.
- (9) (a) Frayssé, S.; Coudret, C.; Launay, J. P. *J. Am. Chem. Soc.* **2003**, *125*, 5880. (b) Hortholary, C.; Coudret, C. *J. Org. Chem.* **2003**, *68*, 2167. (c) Hortholary, C.; Minc, F.; Coudret, C.; Bonvoisin, J.; Launay, J.-P. *Chem. Commun.* **2002**, 1932. (d) Launay, J. P. *Chem. Soc. Rev.* **2001**, *30*, 386. (e) Launay, J. P.; Frayssé, S.; Coudret, C. *Mol. Cryst. Liq. Cryst.* **2000**, *344*, 125. (f) Frayssé, S.; Coudret, C.; Launay, J. P. *Eur. J. Inorg. Chem.* **2000**, 1581. (g) Patoux, C.; Launay, J. P.; Beley, M.; Chodorowski-Kimmes, S.; Collin, J.-P.; James, S.; Sauvage, J.-P. *J. Am. Chem. Soc.* **1998**, *120*, 3717.
- (10) (a) Hage, R.; Prins, R.; Haasnoot, J. G.; Reedijk, J.; Vos, J. G. *J. Chem. Soc., Dalton Trans.* **1987**, 1389. (b) Nieuwenhuis, H. A.; Haasnoot, J. G.; Hage, R.; Reedijk, J.; Snoeck, T. L.; Stufkens, D. J.; Vos, J. G. *Inorg. Chem.* **1991**, *30*, 48. (c) Buchanan, B. E.; Wang, R.; Vos, J. G.; Hage, R.; Haasnoot, J. G.; Reedijk, J. *Inorg. Chem.* **1990**, *29*, 3263. (d) Browne, W. R.; O'Connor, C. M.; Villani, C.; Vos, J. G. *Inorg. Chem.* **2001**, *40*, 5461. (e) Hage, R.; Haasnoot, J. G.; Nieuwenhuis, H. A.; Reedijk, J.; de Ridder, D. J. A.; Vos, J. G. *J. Am. Chem. Soc.* **1990**, *112*, 9245. (f) de Wolf, J. M.; Hage, R.; Haasnoot, J. G.; Reedijk, J.; Vos, J. G. *New J. Chem.* **1991**, *15*, 501. (g) Hage, R.; Dijkhuis, A. H. J.; Haasnoot, J. G.; Prins, R.; Reedijk, J.; Buchanan, B. E.; Vos, J. G. *Inorg. Chem.* **1988**, *27*, 2185. (h) Mehmetaj, B.; Haasnoot, J. G.; De Cola, L.; van Albada, G. A.; Mutikainen, I.; Turpeinen, U.; Reedijk, J. *Eur. J. Inorg. Chem.* **2002**, 1765.
- (11) (a) Barigelletti, F.; De Cola, L.; Balzani, V.; Hage, R.; Haasnoot, J. G.; Reedijk, J.; Vos, J. G. *Inorg. Chem.* **1989**, *28*, 4344. (b) van Diemen, J. H.; Hage, R.; Haasnoot, J. G.; Lempers, H. E. B.; Reedijk, J.; Vos, J. G.; de Cola, L.; Barigelletti, F.; Balzani, V. *Inorg. Chem.* **1992**, *31*, 3518. (c) Barigelletti, F.; De Cola, L.; Balzani, V.; Hage, R.; Haasnoot, J. G.; Reedijk, J.; Vos, J. G. *Inorg. Chem.* **1991**, *30*, 641.
- (12) Browne, W. R.; Weldon, F.; Guckian, A.; Vos, J. G. *Collect. Czech. Chem. Commun.* **2003**, *68*, 1467.
- (13) Passaniti, P.; Browne, W. R.; Lynch, F. C.; Hughes, D.; Nieuwenhuyzen, M.; James, P.; Maestri, M.; Vos, J. G. *Dalton* **2002**, 1740.

in synthetic procedures were of reagent grade or better. *cis*-[Ru(bpy)₂Cl₂]₂·2H₂O¹⁴ and *cis*-[Os(bpy)₂Cl₂]₂·2H₂O¹⁵ were prepared by literature procedures. The ligands 1,3-bis(5-(2-pyridyl))-1*H*-1,2,4-triazol-3-yl)benzene (H₂mL) and 1,4-bis(5-(2-pyridyl))-1*H*-1,2,4-triazol-3-yl)benzene (H₂pL) were prepared using standard methods normally used for the synthesis of pyridyltriazole ligands.^{11a} Detailed synthetic procedures are available as Supporting Information.

H₂mL. Characterization: mp 320–322 °C. ¹H NMR [(CD₃)₂SO]: δ (ppm) 8.88 (1H, s, phenyl H₂), 8.16 (2H, d, phenyl H₄, H₆, *J* = 7.9 Hz), 7.65 (1H, t, phenyl H₅, *J* = 7.9 Hz), 8.23 (1H, d, pyridyl H₃, *J* = 7.9 Hz), 8.02 (1H, dd, pyridyl H₄, *J* = 7.9 Hz), 7.55 ppm (1H, dd, pyridyl H₅, *J* = 6 Hz), 8.72 (1H, d, pyridyl H₆, *J* = 5 Hz), 14.90 (1H, s (broad), H_{NH}). ¹³C NMR [(CD₃)₂SO]: δ (ppm) 121.53, 123.38, 123.62, 125.06, 126.58, 129.41, 131.40, 137.80, 146.31, 149.52, 149.72. Elemental anal. Calcd for C₂₀H₁₄N₈: C, 65.56; H, 3.85; N, 30.59. Found: C, 65.39; H, 3.76; N, 30.57.

H₂pL. Characterization: mp >300 °C. ¹H NMR [(CD₃)₂SO]: δ (ppm) 8.23 (2H, s, phenyl H), 8.19 (1H, d, pyridyl H₃ *J* = 7.9 Hz), 8.02 (1H, dd, pyridyl H₄, *J* = 7.9 Hz), 7.54 (1H, dd, pyridyl H₅, *J* = 6 Hz), 8.72 (1H, d, pyridyl H₆, *J* = 5 Hz), 14.50 (1H, s (broad), H_{NH}). ¹³C NMR [(CD₃)₂SO]: δ (ppm) 121.52, 123.21, 125.11, 126.40, 126.81, 127.45, 137.88, 149.69, 150.41. Elemental anal. Calcd for C₂₀H₁₄N₈: C, 65.56; H, 3.85; N, 30.59. Found: C, 65.83; H, 3.94; N, 30.28.

[Ru(bpy)₂(HmL)]PF₆·H₂O (mRu). H₂mL (0.732 g, 2 mmol) was dissolved in DMF/H₂O (2:1 v/v). *cis*-[Ru(bpy)₂Cl₂]₂·2H₂O (0.39 g, 0.75 mmol) was added to the solution, which was heated at reflux for 8 h. Upon cooling, the solution was filtered to remove unreacted ligand. A few drops of a saturated aqueous NH₄PF₆ solution were added, and the DMF/H₂O was removed by evaporation under reduced pressure. The resulting solid was recrystallized by slow evaporation from acetone/water (2:1 v/v).

All complexes reported in this Communication were purified by column chromatography on neutral alumina unless otherwise stated. The mononuclear compounds contained dinuclear complex as the main impurity and vice versa. Purification by chromatography on neutral Al₂O₃ gave an excellent separation of bands associated with the mononuclear and dinuclear species, respectively. The dinuclear complexes were eluted using acetonitrile, while the mononuclear complexes, which remained at the top of the column, were eluted by the addition of methanol (50–100%) to the mobile phase.

mRu was isolated as the hexafluorophosphate salt and recrystallized from acetone/water (2:1 v/v) to which a few drops of aqueous NH₄OH were added. Yield = 0.32 g (45%). Elemental anal. Calcd for Ru₁C₄₀H₃₁N₁₂O₃P₂F₁₂: C, 50.98; H, 3.26; N, 17.84. Found: C, 50.62; H, 3.60; N, 17.54.

[(Ru(bpy)₂(mL))(PF₆)₂·5H₂O (mRuRu). *cis*-[Ru(bpy)₂Cl₂]₂·2H₂O (0.52 g, 1 mmol) and H₂mL (0.146 g, 0.4 mmol) were dissolved in DMF/H₂O (2:1 v/v), and the mixture was heated at reflux for 4 h. Following the addition of a few drops of a saturated aqueous solution of NH₄PF₆, the reaction mixture was evaporated to dryness under reduced pressure. The resulting solid was purified as described for **mRu**. Yield = 0.515 g (87%). Elemental anal. Calcd for Ru₂C₆₀H₅₄N₁₆O₅P₂F₁₂: C, 45.82; H, 3.46; N, 14.25. Found: C, 46.09; H, 3.43; N, 14.08. Mass spectrometry, EI-MS: [(Ru(bpy)₂(mL))₂]²⁺, found 595.5, theoretical 595.5; [(Ru(bpy)₂(mL))(PF₆)⁺], found 1336, theoretical 1336.

[Os(bpy)₂(HmL)]PF₆·H₂O (mOs). H₂mL (0.30 g, 0.82 mmol) and *cis*-[Os(bpy)₂Cl₂]₂·2H₂O (0.183 g, 0.30 mmol) were dissolved in hot DMF/H₂O (4:1 v/v). A small amount of zinc metal was added to reduce any [Os(bpy)₂Cl]₂ present in the *cis*-[Os(bpy)₂Cl₂]₂·2H₂O starting material, and the reaction mixture was allowed to reflux for 8 h. The solution was cooled and filtered to remove unreacted ligand and the zinc metal. Following evaporation of the solvent, the crude product was dissolved in dichloromethane and any residual [Os(bpy)₂Cl]₂ present removed by filtration. The resulting solid was purified as described for **mRu**. Yield = 0.12 g (40%). Elemental anal. Calcd for Os₁C₄₀H₃₁N₁₂O₃P₂F₆: C, 46.60; H, 3.03; N, 16.30. Found: C, 46.42; H, 3.14; N, 16.09.

[(Os(bpy)₂(mL))(PF₆)₂·4H₂O (mOsOs). This complex was prepared as described for **mOs**. The crude product was purified and recrystallized as described for **mRu**. Yield = 0.12 g (36%). Elemental anal. Calcd for Os₂C₆₀H₅₂N₁₆O₄P₂F₁₂: C, 41.62; H, 3.03; N, 12.94. Found: C, 41.72; H, 3.08; N, 12.81.

[Ru(bpy)₂Os(bpy)₂(mL)](PF₆)₂·3H₂O (mRuOs). [Ru(bpy)₂(HmL)]PF₆ (0.10 g, 0.11 mmol), *cis*-[Os(bpy)₂Cl₂]₂·2H₂O (0.067 g, 0.12 mmol), and a small amount of zinc metal were dissolved in 50 cm³ of methanol/ethanol/water (2:1:1 v/v). The mixture was heated at reflux temperature for 8 h. The progress of the reaction was monitored using the analytical HPLC system. When all the *cis*-[Os(bpy)₂Cl₂]₂·2H₂O had reacted, the solution was filtered to remove the zinc metal and then concentrated to ~15 cm³. A few drops of a saturated aqueous NH₄PF₆ solution were added. The product was collected by filtration and recrystallized from acetone/water (1:1 v/v). The resulting solid was purified as described for **mRu**. Yield = 70 mg (41%). Elemental anal. Calcd for Ru₁-Os₁C₆₀H₅₀N₁₆O₃P₂F₁₂: C, 44.34; H, 3.10; N, 13.79. Found: C, 44.15; H, 2.93; N, 13.46. Mass spectrometry, EI-MS: [Ru(bpy)₂(mL)Os(bpy)₂]²⁺, found 640, theoretical 640.

[Ru(bpy)₂(H₂pL)](PF₆)₂·3H₂O (pRuH). H₂pL (0.732 g, 2 mmol) was dissolved in 150 cm³ H₂O, acidified by addition of 2 M sulfuric acid, and to this was added *cis*-[Ru(bpy)₂Cl₂]₂·2H₂O (0.416 g, 0.8 mmol) slowly. The solution was heated at reflux for 8 h. After this period, the orange solution was neutralized by addition of concentrated NaOH and the volume reduced to 50 cm³. Na₂SO₄ was removed by filtration, and a few drops of a saturated aqueous NH₄PF₆ solution was added to form the PF₆ salt. This product was collected by filtration and recrystallized from acetone/water (1:1 v/v). Purification of the product was carried out by semipreparative HPLC using 80:20 CH₃CN/H₂O containing 0.12 M KNO₃ as the mobile phase. Yield = 0.295 g (40%). Elemental anal. Calcd for Ru₁C₄₀H₃₆N₁₂O₃P₂F₁₂: C, 42.74; H, 3.20; N, 14.95. Found: C, 42.78; H, 3.06; N, 14.96.

[(Ru(bpy)₂(pL))(PF₆)₂·3H₂O (pRuRu). [Ru(bpy)₂(HpL)]PF₆ (0.30 g, 0.32 mmol) and *cis*-[Ru(bpy)₂Cl₂]₂·2H₂O (0.166 g, 0.32 mmol) were dissolved in a methanol/ethanol/water (2:1:1 v/v/v) mixture, and the solution was heated at reflux for 5 h. The reaction mixture was concentrated to 15 cm³, and a few drops of a saturated solution of aqueous NH₄PF₆ were added. The resulting precipitate was filtered off and recrystallized from acetone/water (2:1 v/v). The resulting solid was purified as described for **mRu**. Yield = 0.22 g (45%) Elemental anal. Calcd for Ru₂C₆₀H₅₀N₁₆O₃P₂F₁₂: C, 46.90; H, 3.28; N, 14.59. Found: C, 47.07; H, 3.34; N, 14.48. Mass spectrometry, EI-MS: [(Ru(bpy)₂(pL))₂]²⁺, found 595.5, theoretical 595.5; [(Ru(bpy)₂(pL))(PF₆)⁺], found 1336, theoretical 1336.

[Os(bpy)₂(HpL)]PF₆·3H₂O (pOs). This complex was prepared as described for **mOs**. The resulting solid was purified as described for **mRu**. Yield = 0.20 g (40%). Anal. Calcd for Os₁C₄₀H₃₅N₁₂O₃P₁F₆: C, 45.04; H, 3.28; N, 15.75. Found: C, 45.00; H, 3.02; N, 15.56.

(14) Sullivan, B. P.; Salmon, D. J.; Meyer, T. J. *Inorg. Chem.* **1978**, *17*, 3334.

(15) Buckingham, D. A.; Dwyer, F. P.; Goodwin, H. A.; Sargeson, A. M. *Aust. J. Chem.* **1964**, *17*, 325.

[(Os(bpy)₂)₂(pL)](PF₆)₂·4H₂O (pOsOs). This complex was prepared as described for mOsOs. The resulting solid was purified as described for mRu. Yield = 0.16 g (44%). Elemental anal. Calcd for Os₂C₆₀H₅₂N₁₆O₄P₂F₁₂: C, 41.62; H, 3.03; N, 12.94. Found: C, 41.62; H, 3.06; N, 12.62. Mass spectrometry, EI-MS: [(Os(bpy)₂)₂(pL)]²⁺, found 684.5, theoretical 684.5.

[Ru(bpy)₂Os(bpy)₂(pL)](PF₆)₂·3H₂O (pRuOs). This complex was prepared as described for mRuOs from [Ru(bpy)₂(HpL)]PF₆ (0.10 g, 0.13 mmol) and *cis*-[Os(bpy)₂Cl₂]·2H₂O (0.08 g, 0.13 mmol). The resulting solid was purified as described for mRu. Yield = 0.10 g (50%). Elemental anal. Calcd for Ru₁Os₁C₆₀H₅₀N₁₆O₃P₂F₁₂: C, 44.35; H, 3.10; N, 13.79. Found: C, 44.51; H, 3.03; N, 13.70. Mass spectrometry, EI-MS: [Ru(bpy)₂(pL)Os(bpy)₂]²⁺, found 640, theoretical 640.

Nuclear Magnetic Resonance. ¹H NMR spectra were recorded on a Bruker AC400 (400 MHz) instrument. The solvents used were *d*₆-DMSO for ligands and *d*₃-acetonitrile or *d*₆-acetone for complexes. The chemical shifts were recorded relative to TMS. The spectra were converted from their free induction decay (FID) profiles using a Bruker WINNMR software package.

Absorption and Emission Measurements. UV/visible spectra were obtained using a Shimadzu UV3100 UV-vis-NIR spectrophotometer interfaced to an Elonex PC433 personal computer. Extinction coefficients are ±5%. Emission spectra in the range 500–850 nm were obtained on a Perkin-Elmer LS50-B luminescence spectrometer equipped with a red sensitive Hamamatsu R928 detector, interfaced with an Elonex PC466 personal computer employing Perkin-Elmer FL WinLab custom built software. At room temperature, excitation and emission slit widths of 10 nm were employed. At 77 K measurements were carried out in ethanol/methanol (4:1 v/v) using excitation and emission slit widths of 5 nm. The spectra were not corrected for the photomultiplier response. To ensure protonation/deprotonation, a few drops of perchloric acid or NH₃/diethylamine solution were added to the sample.

Luminescent Lifetime Measurements. Three different methods were used to obtain the emission lifetimes. Below 20 ns fluorescence lifetimes were measured with a time-correlated single-photon counting setup described elsewhere.¹⁶ Briefly, the samples were excited with 150 fs laser pulses at 400 nm with a repetition frequency of 200 kHz. The emission was detected using several alternative filters. For the Ru-based emission, a 600 nm interference filter was used for the acid forms of the complexes and a 695 nm cutoff for the base forms. For the Os-based emission, cutoff filters at 715 and 780 nm were used for the acid and base forms, respectively. The instrumental response function (fwhm) was ca. 120 ps, as determined with a scattering sample and a 400 nm interference filter. The samples were prepared in spectroscopic grade acetonitrile (Merck), with an optical density of ca. 0.3 at 400 nm, and were purged with N₂ before and during measurements. Room temperature lifetimes >20 ns were also measured using the third harmonic (355 nm) of a Spectron Q-switched Nd:YAG spectrum laser system. Emission was detected in a right angled configuration to the laser using an Oriel model IS520 gated intensified CCD coupled to an Oriel model MS125 spectrograph. Room temperature lifetimes were carried out in acetonitrile, unless otherwise stated. The samples used were all of low concentration (10⁻⁴–10⁻⁵ M), and degassing was carried out by bubbling nitrogen through the sample for at least 20 min. Luminescent lifetimes at 77 K were measured using an Edinburgh Analytical Instruments nF900 TCSPC described elsewhere.^{10d} The lifetime are estimated to be ±10%. Good agreement between the three methods was obtained.

Förster Energy Transfer Calculations. The Förster energy transfer rate constants were calculated from eq 1.¹⁷ The following

$$k_{\text{EnT}} = (8.79 \times 10^{-25})(\Phi_{\text{D}}\kappa^2/\tau_{\text{D}}n^4r^6)J \text{ s}^{-1} \quad (1)$$

values were used in these calculations: $r = 1.3 \times 10^{-7}$ cm (13 Å); $\Phi_{\text{D}}/\tau_{\text{D}} = 1 \times 10^5 \text{ s}^{-1}$ and $1.7 \times 10^4 \text{ s}^{-1}$ for the protonated and unprotonated forms, respectively; and $n = 1.344$. The spectral overlap integrals were calculated as $J = 4 \times 10^{-14} \text{ M}^{-1} \text{ cm}^3$ and $J = 4.3 \times 10^{-14} \text{ M}^{-1} \text{ cm}^3$ for the protonated and unprotonated forms, respectively. $\kappa^2 = 2/3$ for a sample of randomly oriented dipoles. In the present case the geometry of the complexes will exclude orientations where the dipoles are oriented along the interdipole axes, so that κ^2 is not likely to be higher than $2/3$. A detailed calculation of κ^2 would require information of the rotational force fields in the molecules. After inspection of rotational geometries possible, however, we estimate that κ^2 is not likely to lie outside the range 0.25–0.75, which gives an accuracy sufficient for the present discussion.

Electrochemistry. Cyclic voltammetry was carried out using a CH instruments model 660 electrochemical workstation interfaced to an Elonex 486 PC. A scan rate of 100 mV s⁻¹ was used for electrochemical measurements. HPLC grade solvents dried over molecular sieves were used. The electrolyte was 0.1 M tetraethylammonium perchlorate (TEAP). The electrochemical cell used was a conventional three-compartment cell with glass frits. The reference electrode used was a saturated calomel electrode (SCE). Ferrocene was used as an internal reference. Its potential was taken to be +0.38 V vs SCE.^{18,19} The working electrode was a 3 mm diameter Teflon shrouded glassy carbon electrode, and a platinum wire was used as the counter electrode. Prior to cathodic measurements the solutions were degassed for 15 min with nitrogen. Protonation and deprotonation of the complexes was achieved by addition of perchloric acid or NH₄OH, respectively.

High Performance Liquid Chromatography. Analytical HPLC experiments were carried out using a Waters HPLC system, consisting of a model 501 pump, a 20 μL injector loop, a Partisil SCX radial PAK cartridge mounted in a radial compression Z module, and a 990 photodiode array detector. The detection wavelength used was 280 nm, and the mobile phase used was 80:20 CH₃CN:H₂O containing 0.1 M LiClO₄ and a flow rate of 2.0 mL/min. Semipreparative HPLC was carried out using an ACS pump, a 1 mL injection loop, and a Waters Partisil SCX 10 μm cation exchange column (25 × 100 mm). The mobile phase used was 80:20 CH₃CN:H₂O containing KNO₃ (0.12–0.20 M). The flow rate used varied between 1.5 and 2.0 mL/min.

pK_a values were determined in Britton–Robinson buffer (0.04 M boric acid, 0.04 M acetic acid, 0.04 M phosphoric acid). The pH was adjusted by adding concentrated NaOH or concentrated H₂SO₄ and was measured using a Corning 240 digital pH meter. The *pK_a* values were determined from the point of inflection of the absorbance versus pH plot.

Mass spectra were obtained using a Bruker-Esquire LC 00050 electrospray ionization mass spectrometer at positive polarity with cap-exit voltage of 167 V. Spectra were recorded in the scan range 50–2200 *m/z* with an acquisition time of between 300 and 900 μs and a potential of between 30 and 70 V. Each spectrum was recorded by summation of 20 scans.

Elemental analyses were carried out by the Microanalytical laboratories at University College Dublin.

(17) Förster, Th. *Discuss. Faraday Soc.* **1959**, 27, 7.

(18) Chang, J. P.; Fung, E. Y.; Curtis, J. C. *Inorg. Chem.* **1986**, 25, 4233.

(19) Connelly, N. G.; Geiger, W. E. *Chem. Rev.* **1996**, 96, 877.

(16) Fanni, S.; Weldon, F. M.; Hammarström, L.; Mukhtar, E.; Browne, W. R.; Keyes, T. E.; Vos, J. G. *Eur. J. Inorg. Chem.* **2001**, 529.

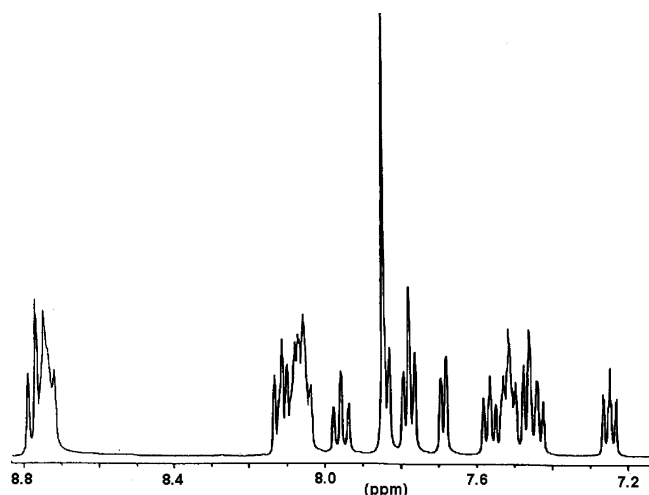


Figure 2. ^1H NMR spectrum of **mRuRu** in d_6 -DMSO.

Results and Discussion

Synthesis. The compounds were prepared using literature methods.¹⁰ However, as described in the Experimental Section under the synthetic procedure for **mRu**, purification of the products obtained is needed to separate the mononuclear from the dinuclear compounds. The dinuclear complexes can be prepared either by using a ligand: $[\text{M}(\text{bpy})_2\text{Cl}_2]\cdot 2\text{H}_2\text{O}$ ratio of 1:2 or, alternatively, by an indirect route from the appropriate mononuclear complexes (complexes as ligands approach²⁰). This latter method is especially useful for the synthesis of the RuOs heterodinuclear compounds. ^1H NMR spectroscopy, together with mass spectral analysis, was employed to confirm the absence of mono/dinuclear impurities in the dinuclear complexes. Elemental analysis and spectroscopic characterization show that, as has been observed for other pyridyltriazole complexes, the ligands H_2mL and H_2pL deprotonate upon coordination of the metal center.²¹ The one exception is **pRu**, which was obtained as the dication since this compound was isolated from an acidic solution. In the mononuclear compounds the free pyridyltriazole arm is protonated, thereby yielding complexes with an overall +1 charge. The protonation state of the solid material obtained is, however, irrelevant in regard to physical measurements carried out as sufficient acid or base is added to ensure protonation/deprotonation, respectively.²²

^1H NMR Spectroscopy. ^1H NMR spectra were obtained for all compounds to confirm the molecular structure of the compounds obtained. The spectrum of **mRuRu** is shown in Figure 2 as a representative example.^{13,23,24} The relative simplicity of the ^1H NMR spectra obtained for the homodinuclear complexes reflects the symmetric environment of the metal centers. For the mononuclear complexes the spectra

are more complicated due to the presence of resonances for both the free and bound pyridyltriazole arms. A full assignment of the triazole-based ligands is available as Supporting Information (See Tables S1 and S2). In the compounds obtained the metal centers may be bound to the triazole moiety via N1 or N4 of the triazole ring (see Figure 1). Analysis of the ^1H NMR data obtained for both mononuclear and dinuclear complexes and comparison of the chemical shifts observed for N1-bound complexes of other similar pyridyltriazole-based systems indicate that coordination takes place via N1.^{12,25} Crystal structures of analogous pyridyltriazole complexes containing the ligands 3-methyl-5-(2-pyridyl)-4H-1,2,4-triazole²⁶ and 3-(2-hydroxyphenyl)-5-(2-pyridyl)-4H-1,2,4-triazole²⁷ also indicate that the $\text{Ru}(\text{bpy})_2$ unit is coordinated via N1. Considering steric considerations this finding is not surprising.¹⁰

Electrochemical Properties. The electrochemical and spectroelectrochemical properties of the homonuclear ruthenium based complexes are reported in depth in an earlier contribution and will be discussed only briefly here.¹² The oxidation and reduction potentials of all complexes are given in Table 1. The waves in the anodic region of the cyclic voltammograms are assigned to metal-centered oxidation processes.²⁸ The protonated complexes, obtained by addition of a few drops of HClO_4 to the solution, show an anodic shift of between 250 and 300 mV compared to their deprotonated analogues. The oxidation potentials of the osmium compounds are approximately 400 mV less positive than observed for the analogous ruthenium complexes, due to the lower binding energy of the Os(II) 5d orbitals compared with the Ru(II) 4d orbitals.²⁹ The reduction waves observed for all the complexes have been assigned as bpy-based by comparison with related compounds,²⁸ the 1,2,4-triazole ligands being weaker π -acceptors than bpy. The homodinuclear RuRu complexes show a single two electron redox wave at 0.84 V vs SCE without any evidence of splitting (<20 mV).¹² This is indicative of an, at best, weak interaction between the two metal centers in the ground state. The fact that the oxidation potentials of the Os(II) and Ru(II) centers in their respective mononuclear and dinuclear complexes are identical, within experimental uncertainty, is in agreement with this observation. Spectroelectrochemical investigations on the compounds were also carried out. The spectroscopic features of the Ru(III) and Os(III) species are as expected and are listed in Table S3.

The spectro-electrochemical features of the intervalence compounds **pRu(II)Ru(III)** and **mRu(II)Ru(II)** were reported in an earlier contribution.¹² For **pRu(II)Ru(III)** an intervalence band was observed at approximately 8000 cm^{-1} ,

(20) Serroni, S.; Campagna, S.; Puntoriero, F.; Di Pietro, C.; McGlenaghan, N. D.; Loiseau, F. *Chem. Soc. Rev.* **2001**, *30*, 367.

(21) Hage, R. Ph.D. Thesis, Leiden University, 1991.

(22) Browne, W. R.; Heseck, D.; Gallagher, J. F.; O'Connor, C. M.; Killeen, J. S.; Aoki, F.; Ishid, H.; Inoue, Y.; Villani, C.; Vos, J. G. *Dalton* **2003**, 2597.

(23) Belser, P.; von Zelewsky, A. *Helv. Chim. Acta* **1980**, *63*, 1675.

(24) Constable, E. C.; Lewis, J. *Inorg. Chim. Acta* **1983**, *70*, 251.

(25) Ryan, E. M.; Wang, R.; Vos, J. G.; Hage, R.; Haasnoot, J. G. *Inorg. Chim. Acta* **1993**, *208*, 49.

(26) Buchanan, B. E.; Vos, J. G.; Kaneko, M.; van der Putten, W. J. M.; Kelly, J. M.; Hage, R.; de Graaff, R. A. G.; Prins, R.; Haasnoot, J. G.; Reedijk, J. *J. Chem. Soc., Dalton Trans.* **1990**, 2425.

(27) Hage, R.; Haasnoot, J. G.; Reedijk, J.; Wang, R.; Ryan, E. M.; Vos, J. G.; Spek, A. L.; Duisenberg, A. J. M. *Inorg. Chim. Acta* **1990**, *174*, 77.

(28) Juris, A.; Balzani, V.; Barigelli, F.; Campagna, S.; Belser, P.; von Zelewsky, A. *Coord. Chem. Rev.* **1988**, *84*, 85.

(29) Goldsby, K. A.; Meyer, T. J. *Inorg. Chem.* **1984**, *23*, 3002

Table 1. Redox Properties^a

	$E_{1/2}$ M(II)/(III)	$E_{1/2}$ ligand		$E_{1/2}$ M(II)/(III)	$E_{1/2}$ ligand
mRu^b	0.84	-1.45, -1.60	mRuH	1.18	-1.47
mOs	0.48	-1.39, -1.71	mOsH	0.76	-1.46 (irr)
mRuRu^b	0.84	-1.40, -1.69	mRuRuH	1.18	-1.53
mOsOs	0.48	-1.41, -1.71	mOsOsH	0.72	-1.43, -1.71 (irr)
mRuOs	0.47, 0.83	-1.44, -1.60	mRuOsH	0.76, 1.16	-1.56 (irr), -1.72 (irr)
pRu^b	0.84	-1.45, -1.61	pRuH	1.15	-1.47
pOs	0.49	-1.37, -1.54	pOsH	0.75	-1.48 (irr), -1.69
pRuRu^b	0.84	-1.50, -1.71 (irr)	pRuRuH	1.14	-1.52, -1.79 (irr)
pOsOs	0.49	-1.36, -1.52, -1.75	pOsOsH	0.73	-1.39, -1.66
pRuOs	0.48, 0.85	-1.47, -1.68 (irr)	pRuOsH	0.73, 1.14	-1.47, -1.60 (irr)

^a Oxidation and reduction potentials of the mononuclear and dinuclear complexes with H₂mL and H₂pL (V vs SCE). All measurements carried out in acetonitrile with 0.1 M TEAP. ^b From ref 12.

Table 2. Absorption and Emission Data^a

complex	absorbance λ_{\max} , nm ($10^{-4}\epsilon$)	emission λ_{\max} , nm 300 K	lifetime, ns at 300 K ^c	emission λ_{\max} , nm 77 K	lifetime (ns) at 77 K ^b
mRu	482 (0.85)	688	117	612	3150
mRuH	440	613	2.5 (60); 10 (40)	578	5200
mRuRu	482 (2.00)	687	115	618	2600
mRuRuH	440	611	2.5 (50); 10 (50)	581	4800
mOs	503 (1.13), 652 (0.23)	813	23	759	
mOsH	576, 468, 431	726	38	719	
mOsOs	502 (2.20), 660 (0.49)	811	<20	759	
mOsOsH	679, 472, 431	736	46	711	
mRuOs	485 (1.95), 660 (0.22)	688, 806	6.3 ^d	615, 750	10, ^d 305 ^e
mRuOsH	565, 431	727	1.0 (50), 3.0 (50); ^d 38 ^e	581 (w), 705	5, ^d 855 ^e
pRu	482 (0.98)	685	110	610	3200
pRuH	432	612	2.5 (60); 6 (40)	580	4950
pRuRu	481 (2.03)	690	100	610	2800
pRuRuH	420	614	2.5 (60); 6 (40)	584	4700
pOs	501 (1.05), 644 (0.22)	814	<20	761	
pOsH	576, 463, 427	737	34	720	
pOsOs	502 (2.43), 648 (0.53)	814	6	753	
pOsOsH	581, 429	725	45	718	
pRuOs	483 (2.25), 629 (0.35)	684, 795	5.7 ^d	615 (w), 750	10, ^d 325 ^e
pRuOsH	568, 424	725	0.6; 37 ^e	585, 710	5, ^d 740 ^e

^a Unless otherwise stated, all measurements were carried out in acetonitrile. Protonation of the complexes was achieved by the addition of perchloric acid. ^b Measured in 4/1 ethanol/methanol. ^c Samples deoxygenated using N₂. For biexponential decays the contribution of each component is given in parentheses. ^d Ru(II). ^e Os(II)-based emission.

but no such feature was observed in the **mRu(II)Ru(III)** analogue. No intervalence features were observed for the protonated species **pRu(II)Ru(III)H** and **mRu(II)Ru(III)-H**. These observations further confirm that the interaction between the two metal centers in these dinuclear compounds is very weak. The fact that, for the protonated compounds, no intervalence features are observed suggests for the present system a superexchange hole transfer interaction (vide infra). The absence of an intervalence band in the absorption spectrum of **mRu(II)Ru(III)** is in agreement with the expected reduced electronic coupling for meta- vs para-based systems.¹² Similarly, during the oxidation of **pOsOs**, a weak band at 9400 cm⁻¹ appears and subsequently disappears during the course of the oxidation but no such bands are observed for the **mOsOs** or their protonated forms

In contrast to the homoleptic complexes, where the absence of a separation between the first and second metal oxidation processes renders generation of the mixed valence species difficult, for the heteroleptic complexes the large separation ($\Delta E < 350$ mV) between the Os(II)- and Ru(II)-based oxidations results in a very high comproportionation constant (K_c) for the mixed valent Ru(II)Os(III) species, and hence generation of the Ru(II)Os(III) oxidation state is rendered

more straightforward. No evidence of an intervalence transition was observed for **mRuOs**, **mRuOsH**, or **pRuOsH**. Surprisingly for **pRuOs** no intervalence transitions were observed. Due to the redox asymmetry of the mixed-metal system, it is expected that the energy of an IVCT band for **pRuOs** would be higher than ν_{\max} for the analogous **pRuRu** complex.^{30,31} The intervalence band, if present, would therefore be masked by the Os(III) LMCT bands.

Electronic Properties. Electronic absorption and emission data for the complexes in their protonated and deprotonated forms are presented in Table 2. The electronic absorption spectra of all the complexes are dominated in the visible region by $d\pi-\pi^*$ metal-to-ligand charge transfer (MLCT) transitions typical of complexes of this type and in the UV region (250–350 nm) by intense ligand-based $\pi-\pi^*$ transitions associated with the 2,2'-bipyridyl and bridging ligands.

(30) Richter, M. M.; Brewer, K. J. *Inorg. Chem.* **1993**, 32, 2827.

(31) Using the relationship (eqs a and b) between intervalence absorption energies ($\Delta\nu_{\max}$) and the difference in redox potentials ($\Delta(\Delta E_{1/2})$) devised by Goldsby and Meyer,²⁹ an intervalence charge transfer band associated with **pRuOs** would be predicted to occur around 950 nm.

$$\Delta\nu_{\max} = \Delta(\Delta E_{1/2}) = \Delta E_{1/2}(\text{Ru/Os}) - \Delta E_{1/2}(\text{Ru/Ru}) \quad \text{a}$$

$$\Delta\nu_{\max} = \nu_{\max}(\text{Ru}^{\text{II}} - \text{Os}^{\text{III}}) - \nu_{\max}(\text{Ru}^{\text{II}} - \text{Ru}^{\text{III}}) \quad \text{b}$$

Upon protonation of the triazole ring, the ligand (H_2mL/H_2pL) becomes a weaker σ -donor and a stronger π -acceptor, lowering the energy of the metal-based orbitals, which results in the observed blue shift in the absorption spectrum.^{26,32} For the Os(II) complexes, additional absorption bands are observed at 600–660 nm, which can be assigned to formally forbidden triplet $d\pi-\pi^*_{bpy}$ MLCT transitions.³³ The absorption spectra of equimolar solutions of the heterodinuclear complexes **mRuOs** and **pRuOs** and 1:1 mixtures of the corresponding homodinuclear species, **pRuRu/pOsOs** and **mRuRu/mOsOs**, were found to be identical. This indicates that the electronic structure of each metal center in the binuclear complexes is largely independent of the other metal center and hence suggests that, as for ground state interaction (vide supra), excited state intercomponent interaction is, at best, very weak.

As is typical of pyridyltriazole-based Ru(II) and Os(II) complexes, a well-defined acid–base chemistry is observed. The pK_a values obtained are in the range 3.3 ± 0.3 . The values obtained for the individual compounds are given in the Supporting Information (Table S4).^{26,34} It is notable that for the dinuclear species only one pK_a value is obtained.¹³ The absence of a ground state interaction between the two 1,2,4-triazole moieties demonstrates the weakness of the bridging phenyl group in mediating intercomponent interactions. The pK_a values observed for the Os(II)-based homoleptic complexes are only marginally lower than that of the analogous Ru(II)-based complexes (by at most 0.3 pH unit), and hence in the case of the **mRuOs** and **pRuOs**, each of the protonation steps is too close to be distinguished.³⁵

As for the absorption spectra, protonation of the complexes results in a blue shift of the emission maxima (Table 2). The emission maxima obtained at room temperature as well as at 77 K are as expected for this class of compounds.¹¹ No difference is observed between the emission maxima of mononuclear and homodinuclear compounds, again indicating at best a weak interaction between the two metal centers in the dinuclear species.

One initially surprising observation is the different effect that protonation of Ru(II) and Os(II) complexes has on the emission lifetime (Table 2). While the emission energy in all complexes increase upon protonation, the effect of protonation on their emission lifetime is quite different. There is a dramatic *decrease* in the excited state lifetime of the Ru(II) emission, while the Os(II) emission lifetimes are significantly *increased*. The observation can be rationalized by considering the two main factors that control the excited

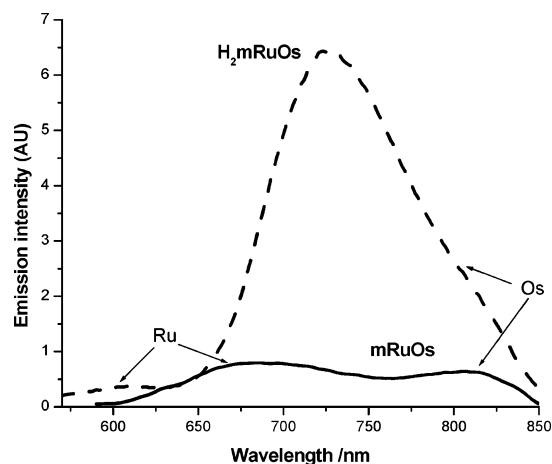


Figure 3. Room temperature emission spectrum for **mRuOs** (solid line) and **mRuOsH** (dashed line) ($\sim 10^{-5}$ M, excitation at the isoabsorptive point). The ruthenium and osmium contributions to the emission envelope are indicated as Ru and Os, respectively.

state lifetime for this type of complex: the energy gap law³⁶ (governed by the energy gap between the ground and emitting states) and the gap between the emitting 3MLCT state and the deactivating 3MC state. For the Ru(II) complexes the latter factor controls most of the excited state decay in the compounds. Protonation of the triazole decreases the σ -donor capacity of the ligand. Consequently the ligand field splitting is decreased, which favors thermal population of the strongly deactivating e_g^* (3MC) state and faster radiationless decay, resulting in shorter lifetimes.³⁷ However, for the Os(II) complexes the strength of the ligand field is large and the 3MC level cannot be populated. As a result the emission lifetime is primarily governed by the energy gap law and, due to the higher 3MLCT energy, the emission lifetime is *increased*.

The time-resolved emission decays for all the protonated mononuclear and homodinuclear Ru(II) complexes are biexponential. The presence of the exponents with approximately equal amplitudes implies that this behavior cannot be due to an impurity (this is apparent from the NMR data and the fact that the same samples in a basic solution gave single exponential decays).

Earlier studies have found that coordination isomers, bound via either the N1 or N4 nitrogen of the 1,2,4-triazole ring (see Figure 7), yield compounds with very different electronic properties.³⁸ Similarly, methylation at either the N2 or N4 position of $[Ru(bpy)_2(pytr)]^+$ also results in complexes exhibiting different electronic properties, in particular differing emission lifetimes.¹⁶ These studies demonstrate the inequivalence of the N1/N2 and N4 positions toward modification; and because only one site may be protonated and neither site is particularly favored above the other, it is probable that in solution an equilibrium mixture of two species {protonated at either the N2 or N4 position} is

(32) Duati, M.; Tasca, S.; Lynch, F. C.; Bohlen, H.; Vos, J. G.; Stagni, S.; Ward, M. D. *Inorg. Chem.* **2003**, *42*, 8377.

(33) Haga, M.; Matsumura-Inoue, T.; Yamabe, S. *Inorg. Chem.* **1987**, *26*, 4148.

(34) Browne, W. R.; O'Connor, C. M.; Hughes, H. P.; Hage, R.; Walter, O.; Doering, M.; Gallagher, J. F.; Vos, J. G. *Dalton* **2002**, 4048.

(35) For the mononuclear complexes it would be expected that a second deprotonation step (due to the unbound 1,2,4-triazole ring) would be observed at higher pH. However, the effect on the absorption spectrum of the complex of deprotonation of such a peripheral group would be expected to be negligible, considering the limited influence that substituents in the C3 position of the 1,2,4-triazole have on the electronic properties of this class of complexes.³⁴

(36) Kober, E. M.; Caspar, J. V.; Lumpkin, R. S.; Meyer, T. J. *J. Phys. Chem.* **1986**, *90*, 3722.

(37) Wang, R.; Vos, J. G.; Schmehl, R. H.; Hage, R. *J. Am. Chem. Soc.* **1992**, *114*, 1964.

(38) Fanni, S.; Keyes, T. E.; O'Connor, C. M.; Hughes, H.; Wang, R.; Vos, J. G. *Coord. Chem. Rev.* **2000**, *208*, 77.

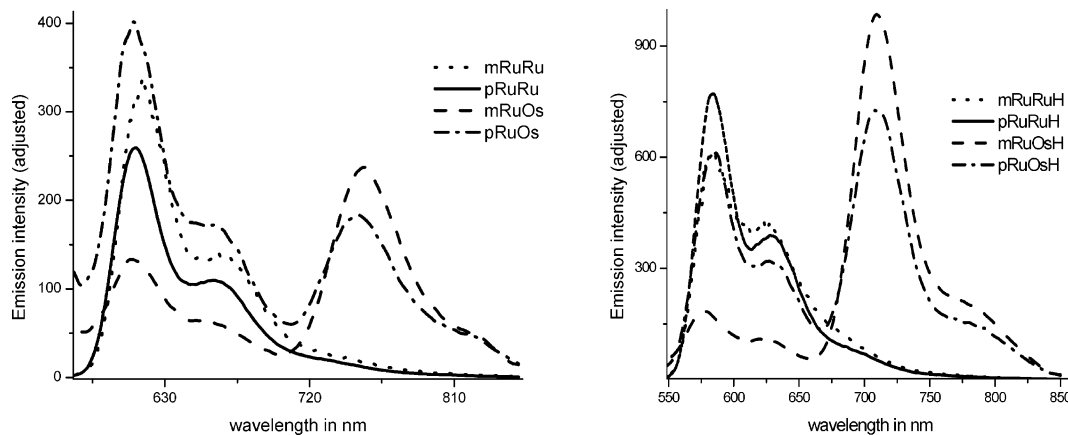


Figure 4. Emission spectrum of dinuclear complexes at 77 K in basic (left) and acidic (right) 5/1 v/v ethanol/methanol (spectral intensity is adjusted for clarity).

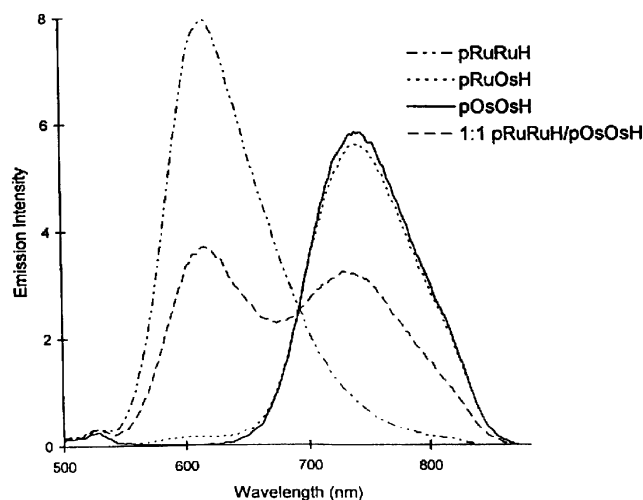


Figure 5. Room temperature emission spectra of **pRuOsH**, **pRuRuH**, and **pOsOsH** and of an equimolar mixture of **pRuRuH** and **pOsOsH** in CH_3CN ($\sim 10^{-5}$ M) (excitation at the isoabsorptive point).

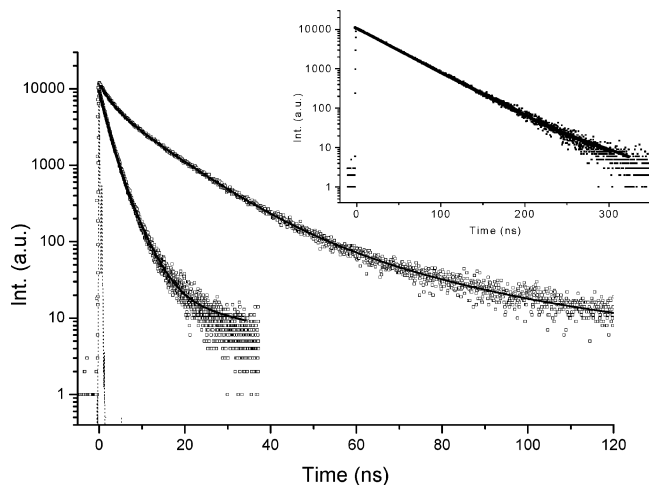
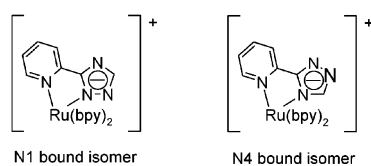


Figure 6. Time-resolved decay of the Ru emission observed at 600 nm for **mRuRuH** (upper curve) and **mRuOsH** (lower curve) in CH_3CN ($\sim 10^{-5}$ M). The dashed line is the instrumental response function. Inset: Decay of the Os-based emission at $\lambda > 715$ nm for **mRuOsH**.

present, i.e., RuH_4 and RuH_2 . Hence two limiting situations are possible: (1) the rate of exchange between N2 and N4 protonation is much faster than the emission decay rate of either species and an averaged lifetime is observed and (2)

Coordination isomers of $[\text{Ru}(\text{bpy})_2(\text{pytr})]^+$



Methylation isomers

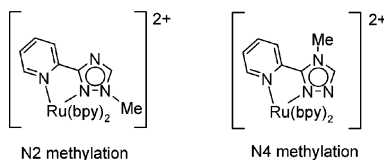


Figure 7. Coordination isomers of mononuclear complexes discussed in text.

the rate of exchange is much slower than the emission decay rate of each center and biexponential behavior is observed. The assumption that RuH_4 and RuH_2 will have different emission lifetimes is not unreasonable since such differences in emission lifetime have been observed for N2 and N4 methylated complexes.¹⁶

In dry acetonitrile, the rate of proton exchange is quite slow and equilibrium may not be established within the emission lifetime. Hence, the biexponential behavior observed for the homonuclear Ru(II) complexes is likely to be due to protonation of inequivalent sites.³⁹ For the Os(II) containing complexes only a monoexponential decay is observed. The absence of a biexponential emission decay may possibly be explained by the much longer emission lifetime for these complexes that allows proton equilibration during the excited state lifetime. Alternatively, the difference between the protonation isomers may be less important for the Os(II) complexes that decay predominantly by internal conversion to the ground state, instead of by activated decay via metal-centered states as for the Ru(II) complexes.

(39) In protic media the rate of proton exchange is expected to be much faster than the lifetime of the excited state and hence an averaged lifetime is observed (i.e., single exponential) and hence addition of protic solvents to the acetonitrile solutions would be expected to result in a monoexponential lifetime being observed. The reduction in emission intensity in the presence of protic solvents, however, makes such experiments ambiguous.

Table 3. Emission Lifetimes and Calculated Energy Transfer Parameters

	τ_{em}/ns		k_{EnT}/s^{-1} ^b		$k_{F\ddot{o}rster}/s^{-1}$ ^c
	Ru-based	Os-based	293 K	77 K	
pRuOs ^a	5.7	<6	1.6×10^8	1×10^8	3×10^7
pRuOsH ^a	0.6	37	$\approx 1.4 \times 10^9$	2×10^8	2×10^8
mRuOs ^a	6.3	<6	1.5×10^8	1×10^8	3×10^7
mRuOsH ^a	≈ 1.0 ($\approx 50\%$); ≈ 3.0 ($\approx 50\%$)	38	$(2-6) \times 10^8$	2×10^8	2×10^8

^a Measured by time-correlated single-photon counting. ^b Calculated from the time-resolved data (see text). ^c Calculated using the parameters given in the Experimental Section.

Intercomponent Interaction in RuOs Compounds. At room temperature both **mRuOs** and **pRuOs** exhibit a weak dual emission with maxima at around 680 and 800 nm. The spectrum observed for **mRuOs** is shown as an example in Figure 3. By comparison with homodinuclear complexes these two emissions may be assigned to the Ru-bound and Os-bound sites, respectively. For both complexes, the emission from the Ru-based component is slightly stronger than that from the Os-based unit. Examination of the emission spectra of the protonated **mRuOsH** (See Figure 3) and **pRuOsH** complexes reveals that in both cases emission from the Os-based site is now the predominant spectral feature. The Ru-based emission appears as a very weak band preceding the tail of the Os(II) luminescence.

At 77 K emission from both sites can be seen. From the luminescence maxima at 77 K, it can be seen that the Ru→Os energy transfer step in **mRuOs** and **pRuOs** is energetically allowed by approximately 0.36 eV. These observations suggest quenching of the Ru(II)-based luminescence via an energy transfer mechanism. Such dual luminescence is unusual, although some well-documented examples have been reported by Barigelletti^{40,41} and co-workers. The relative intensities of the Ru(II) and Os(II) emission for **mRuOs** and **pRuOs** and their protonated forms are, however, more complicated than at 298 K. For **mRuOs**, the Os-based luminescence is found to be twice as intense as the Ru-based luminescence, while for **pRuOs**, the Ru-based emission is more intense than the Os-based luminescence. The emission lifetime data at 77 K (Table 3) show that the Ru-emission is quenched by 99%. A detailed analysis of the difference in the intensity of the ruthenium-based emission in the two types of compounds is precluded because of the sensitivity of the emission intensities to small amounts of unquenched Ru(II) impurities (Figure 4).

To further investigate the dual emission properties, the emission properties of equimolar solutions of homo- and heterodinuclear complexes were investigated at 298 K. The intensity of the Ru-based emission maximum (at wavelengths where Os emission is negligible) was compared for the RuOs and RuRu complexes. In **pRuOs** the Ru emission was only 6% of that in **pRuRu**, revealing a strong quenching by the Os center. Similarly, the Ru emission intensity in **mRuOs**

was only 8% of that in **mRuRu**. Excitation of equimolar solutions of **pRuRuH**, **pOsOsH**, and **pRuOsH** at the isobestic point (457 nm) is shown in Figure 5. The emission spectrum obtained for **pRuOsH** indicates that the Ru-based emission is almost completely quenched, giving only 2% of the intensity in **pRuRuH**. Furthermore, it was found that the Os-based luminescence in **pRuOsH** is as intense as that of an equimolar **pOsOsH** solution, a finding consistent with energy transfer.

The steady state results are reflected in the excited state lifetimes. Figure 6 shows examples of emission traces for **mRuRuH** and **mRuOsH**. In **mRuOs** and **pRuOs** the lifetime of the Ru-based emission at 300 K is much shorter than in the corresponding homodinuclear complexes (Table 2). We attribute the reduction in lifetime to energy transfer to the Os(II) center, consistent with the emission spectral results above. As for the homometallic complexes, the Ru-based emission decay was not single-exponential for **mRuOsH**, presumably due to the presence of two protonation isomers (vide supra). The more short-lived emission in **pRuOsH** ($\tau = 0.6$ ns) appeared single-exponential, possibly because the energy transfer is rapid enough compared to the excited state decay to make the observed lifetime difference between the two emitting centers (i.e., Ru and Os) indistinguishable.

In the protonated complexes **pRuOsH** and **mRuOsH** a more long-lived and single-exponential (ca. 37 ns) Os-based emission is observed. The lifetime of this Os emission is very similar to the emission lifetime of **pOsOsH** and **mOsOsH**. No rise of the Os-based emission due to energy transfer could be observed in the heterodinuclear complexes because the Ru emission was more intense—in terms of number of photons per time unit—even at longer wavelengths. Instead, evidence for sensitization of the Os emission by energy transfer was provided by the steady state emission data above.

In the deprotonated complexes, **pRuOs** and **mRuOs**, a single-exponential ca. 6 ns lifetime was observed at all wavelengths examined (600–800 nm), also with an interference filter at 600 nm where any Os-based emission is negligible. Thus, we attribute the ca. 6 ns component to Ru-based emission. This is ca. 5% of the lifetime for the corresponding **RuRu** complexes, in good agreement with the relative emission yields from the emission spectra above. No Os-based emission could be resolved, however. The emission lifetime of the complex **pOsOs** is ~ 6 ns, and hence the Os-based emission in **pRuOs** is likely to have a lifetime that is accidentally very similar to that for the Ru emission.⁴²

Energy Transfer Mechanism. The experimental rate constant for energy transfer from the Ru(II) to the Os(II) center, k_{EnT} , can be calculated from the difference in Ru emission decay rate in the Ru–Os and the corresponding

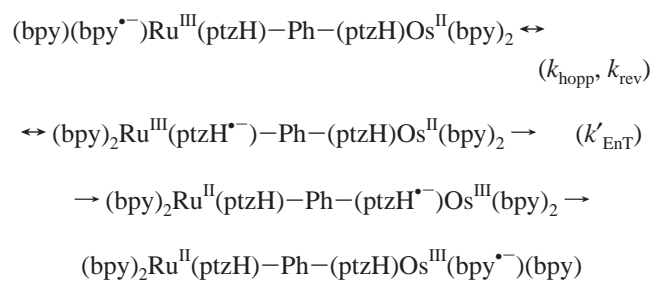
(40) Barigelletti, F.; Flamigni, L.; Guardigli, M.; Juris, A.; Beley, M.; Chodorowski Kimmes, S.; Collin, J.-P.; Sauvage, J.-P. *Inorg. Chem.* **1996**, *35*, 136.

(41) Barigelletti, F.; Flamigni, L.; Collin, J.-P.; Sauvage, J.-P. *Chem. Commun.* **1997**, 333.

(42) For the deprotonated complexes, this emission lies in a region where the detector of the time-resolved single photon counting setup has a very low sensitivity. The Ru-based emission is also comparatively strong—in terms of number of photons per time unit—even in the far-red part of the spectrum. Thus, it is not surprising that an Os-based emission, with a lifetime very similar to that of the Ru emission, cannot be resolved in **pRuOs** and **mRuOs**.

RuRu complex using the equation $k_{\text{EnT}} = 1/\tau_{\text{RuOs}} - 1/\tau_{\text{RuRu}}$. The values obtained in this manner for the different compounds are given in Table 3. In the case of the protonated complexes at room temperature, which exhibit biexponential emission decay, approximate values were calculated by assuming that the more long-lived Ru protonation state also gave the slower energy transfer in the Ru–Os complex. The energy transfer rate constants are very similar at 293 and 77 K, except for **pRuOsH**, where it is an order of magnitude faster at 293 K (see discussion below). Energy transfer is relatively slow in the present complexes compared to other Ru–Os complexes that were linked by phenyl groups but where all ligands were polypyridines, and the lowest MLCT states of the complexes involved the bridging ligands.⁴³ This difference is likely to be due to the localization of the lowest ³MLCT states of both the Ru and the Os centers on the peripheral (bpy) ligands (the ³MLCT states involving the bridging ligand are much higher in energy also in the protonated complexes). This serves to increase the effective energy transfer distance and decreases through-bond coupling. The energy transfer rates in the complexes presented here are instead similar to those reported for a series of phenyl-bridged complexes where the bridging ligands are cyclo-metalating dipyrindinebenzene fragments.⁴⁰ Also in these complexes one may expect that the lowest MLCT states were localized on the peripheral ligands, and that the MLCT states of the bridging ligands are much higher in energy.

The energy transfer in the present complexes can occur either through a direct dipolar coupling (Förster) or by an exchange mechanism (Dexter). In the latter case, the coupling is mediated through bonds and would occur by an interligand hopping of the excited MLCT state. Hopping would give a transient population of the MLCT state of the bridging ligand followed by energy transfer to the Os center:



The exchange mechanism gives two kinetic limits for the overall rate constant k_{EnT} : either the rate of energy transfer when excitation is on the bridging ligand (k'_{EnT}) is much faster than the reverse (downhill) hopping of the MLCT state back to the peripheral ligands of the Ru center (k_{rev}), or alternatively the opposite is true. In the first limit when $k'_{\text{EnT}} \gg k_{\text{rev}}$, the overall rate constant k_{EnT} is limited by the uphill, interligand hopping: $k_{\text{EnT}} = k_{\text{hopp}}$. In the second limit, the overall rate will be proportional to the fractional population of the MLCT state of the bridging ligand; $k_{\text{EnT}} = (k_{\text{hopp}}/k_{\text{rev}})k'_{\text{EnT}}$, i.e., the rate would decrease exponentially with

(43) Barigelletti, F.; Flamigni, L.; Balzani, V.; Collin, J.-P.; Sauvage, J.-P.; Sour, A.; Constable, E. C.; Cargill Thompson, A. M. W. *J. Am. Chem. Soc.* **1994**, *116*, 7692.

increasing energy difference between that state and the peripheral MLCT state.

With these considerations in mind, it is difficult to explain the experimental rate constants by a Dexter-type exchange mechanism alone. First, the rate constant increases only by a factor of 10 or less when the complexes are protonated. The effect of protonation of the triazole ligands would be expected to give a much larger effect on the transient population of the MLCT state of the bridging ligand.⁴⁴ Second, there is no significant difference in the observed energy transfer rate between **pRuOs** and **mRuOs**, while a through-bond coupling is expected to be much weaker in the meta-substituted complex (cf. ground state interaction¹²). Third, the rate constants are very similar at 293 and 77 K (except for **pRuOsH**). While Förster energy transfer should exhibit a very weak temperature dependence, a through-bond Dexter mechanism via activated interligand hopping should show a strong temperature dependence. These results support a mechanism in which the dipole–dipole (Förster) energy transfer is the dominant mechanism for energy transfer.

Calculated Förster rate constants (see Experimental Section and Table 3) are smaller than those obtained experimentally. This inconsistency may be explained by the fact that the Förster calculations are based on the point dipole approximation, while in the present case the MLCT dipoles are quite significantly extended compared to the dipole–dipole separation distance. Nevertheless, the calculations correctly predict that the values for **pRuOs** and **mRuOs** are the same, and they also give a correct estimate (within experimental error) for the relative rates for the protonated and unprotonated complexes. The somewhat larger experimental rate constant for **pRuOsH** than for **mRuOsH** at 293 K may, however, indicate an additional contribution from an exchange mechanism in the former complex. This assignment is supported by the temperature-dependent data: at 77 K the rate constants for **pRuOsH** and **mRuOsH** are equal. This is expected for an essentially temperature-independent Förster mechanism. The activated Dexter energy transfer is instead negligible at 77 K but significant at 293 K for **pRuOsH**. This complex is both protonated and para-substituted, which favors the through-bond energy transfer.

In conclusion, the excited state energy transfer interaction seems to be dominated by through-space Förster contributions. A through-bond Dexter mechanism seems to be significant only in **pRuOsH**. This is in contrast to the ground state interactions, as revealed by electrochemical data and intervalence absorption spectra.¹² These show large differences between the complexes with para- and meta-substituted

(44) In the limit when $k_{\text{EnT}} = (k_{\text{hopp}}/k_{\text{rev}})k'_{\text{EnT}}$, a rate constant increase by a factor of 10 corresponds to only a 60 meV decrease in the energy difference between the MLCT states on the peripheral and the bridging ligands (that determines the ratio $k_{\text{hopp}}/k_{\text{rev}}$). In the limit when $k_{\text{EnT}} = k_{\text{hopp}}$, the effect of changing the energy difference (ΔG_0) can be estimated by the classical Marcus equation. Because MLCT hopping to the bridging ligand is uphill, $d(\ln k_{\text{EnT}})/d(\Delta G_0) < -20 \text{ eV}^{-1}$. A factor of 10 increase in k_{EnT} would then correspond to a <120 meV increase in driving force for the hopping. Clearly, the effect of protonation of the triazole on the energy difference between the MLCT states on the peripheral and the bridging ligands is much larger than both these estimates.

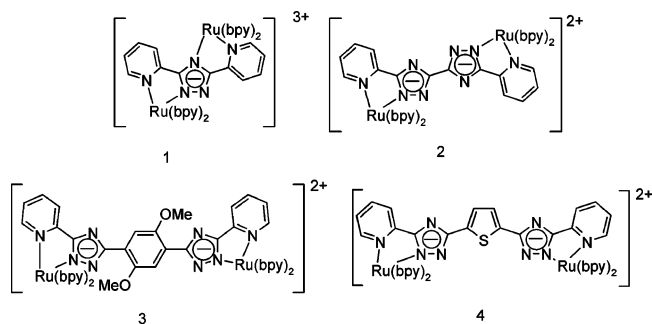


Figure 8. Structures of some related dinuclear compounds.

bridging ligands and between protonated and unprotonated complexes, suggesting a through-bond hole transfer interaction.

Conclusions

The study of the ground and excited state intercomponent interaction in multinuclear complexes incorporating the 1,2,4-triazolato anion has enabled the development of a detailed picture of the mechanisms that mediate such interactions. For compounds based on the different bridging ligands shown in Figure 8, it was observed that ground state interaction via hole transfer is strong for bpt^- type systems (compound **1** in Figure 8), but decreases going from bpt^- to bispytr^{2-} (compound **2**) to the compounds reported here and the dimethoxy analogue (compound **3**) but increases for compound **4**. Significantly, the effect of protonation on the ground state internuclear interaction in all cases is to reduce its strength. Given that protonation results in a lowering of the bridging-ligand HOMO energy and together with the effect of synthetic variation of the HOMO energy by variation of the “spacer” group (i.e., phenyl, dimethoxyphenyl, and thienyl), the nature of ground state interaction can be identified as occurring through a hole transfer mechanism through the bridging ligand HOMO orbitals.¹² The effect of meta vs para coupling on the interaction strength supports the conclusion that a through-bond mechanism is in operation since if a through space mechanism were to be

important then the meta substitution would serve to reduce internuclear separation and hence increase rather than decrease coupling.⁴⁵

From the similarities in absorption, emission, and acid/base properties, it is clear that the electronic structure of each unit in the binuclear complexes is largely unperturbed by the bridging ligand, and hence each unit can be viewed as being a distinct molecular unit rather than a part of a larger “delocalized” molecule. In contrast to ground state interaction, the contribution of a superexchange (through-bond) mechanism for the excited state energy transfer in these systems is much less significant and a through-space mechanism is dominant. For the bpt^- system energy transfer from the Ru(II) to the Os(II) center was found to be efficient with no emission from the ruthenium site being observed. In the compounds reported here (based on the ligands H_2mL and H_2pL), it is evident that the interaction between the metal centers is reduced considerably, resulting in dual emission being observed. The increasing distance between the metal centers can explain this reduced efficiency of energy transfer, and the behavior observed is indicative of a predominantly dipole–dipole (Förster type) mechanism for energy transfer, which may dominate when through-bond coupling is very weak.

Acknowledgment. The authors thank Enterprise Ireland for financial support.

Supporting Information Available: Synthetic procedures for ligands H_2mL and H_2pL . Table S1 containing ^1H NMR data for the complexes with H_2mL . Table S2 containing ^1H NMR data for the complexes with H_2pL . Table S3 containing UV/vis/NIR absorption data for the fully oxidized complexes of H_2mL and H_2pL in their protonated and deprotonated forms. Table S4 containing $\text{p}K_a$ values for the coordinated triazole rings in the complexes. This material is available free of charge via the Internet at <http://pubs.acs.org>.

IC049896P

(45) Liu, T.-Y.; Chen, Y. J.; Tai, C.-C.; Kwan, K. S. *Inorg. Chem.* **1999**, *38*, 674